Optics Communications 300 (2013) 265–268

Contents lists available at SciVerse ScienceDirect

Optics Communications

journal homepage: www.elsevier.com/locate/optcom

A nanoscale refractive index sensor in two dimensional plasmonic waveguide with nanodisk resonator

Alireza Dolatabady, Nosrat Granpayeh *, Vahid Foroughi Nezhad

Optical Communication Lab, Faculty of Electrical and Computer Engineering, K.N. Toosi University of Technology, Tehran, Iran

ARTICLE INFO

Article history:
Received 8 March 2012
Received in revised form
15 February 2013
Accepted 18 February 2013
Available online 6 March 2013

Keywords:
Plasmonic sensor
Refractive index sensor
FDTD method
Nanodisk resonator.

ABSTRACT

In this paper, we have analyzed and simulated the behavior of a nanoscale refractive index sensor in two-dimensional plasmonic waveguide with nanodisk resonator, using the numerical method of finite difference time domain (FDTD). The analytic and simulation results demonstrate the linear correlation between the resonance wavelengths of the nanodisk of the sensor and the refractive index of the material under sensing. The resolution of the sensor depends on the wavelength resolution of the detection system. This sensor can be exploited for identification of various materials, especially as a useful biosensor, by proper design.

1. Introduction

An optical sensor is a sensing structure which, by an optical device, the physical parameter being measured is altered another parameter which is typically encoded into one of the features of a lightwave. One approach to this aim is to use surface plasmon polaritons (SPPs). SPPs are the excited waves on the surface of the metals due to the interaction of the free electrons in metal and incident electromagnetic field in the contiguous dielectric. SPPs are attenuated exponentially in the direction perpendicular to the metal-dielectric interface [1,2]. The aptitude of confinement of light in SPPs beyond the diffraction limit is a revolt in optoelectronic devices and fulfills the dimensions reduction [3]. This offers the sensors with intrinsic improvement to attain high integration. In the past decades, SPP sensors have been widely investigated and studied based on various ideas such as SPP resonance of nanoparticles [4,5], and enhanced transmission through nanohole arrays [6,7]. On the other hand, several sensors based on the surface plasmon resonance (SPR) phenomena have been investigated [8,9]. SPR sensors have created a center of attention and numerous researches have been appeared in their applications. The growing interest in refractive index sensors for industry has increased the necessity for sensitive sensors to detect leaks and distinguish different kinds of materials. In SPR sensors, some resonance modes are excited under particular conditions. These conditions are enormously sensitive to the refractive index of the ambient and the other structural parameters. Some of the SPR sensors detect the variations of the refractive indices of the media. A plasmonic refractive index sensor including cavity structure has been recently proposed [10]. In addition, the refractive indices have relationship with other parameters. Therefore, refractive index sensors are appropriate options for manufacturing various sensors to measure temperature, pressure, humidity and concentration of chemicals [11–15].

In this paper, a novel SPP refractive index sensor based on metal–insulator–metal (MIM) waveguide coupled to a nanodisk resonator is investigated. The sensor performance is simulated numerically by the FDTD method.

This paper is organized as follows. In Section 2, the structure and its analysis method are introduced and the basic principles are analytically presented. In Section 3, the simulation results are discussed and the paper is concluded in Section 4.

2. The structure and theoretical analysis

Our proposed structure is based on the simple nanodisk resonator, shown in Fig. 1. The input and output waveguides are coupled in the resonance frequencies of the nanodisk.

As we will discuss, the resonance wavelengths depend on the refractive indices of the material in the nanodisk resonator. So, the refractive index can be obtained from the resonance wavelengths, and the material can be recognized.

Let us assume that a TM_x plane wave is incident upon a two dimensional circular disk, the incident, scattered and transmitted

* Corresponding author. Tel.: +98 21 84062311; fax: +98 21 88462066.
E-mail addresses: granpayeh@eetd.kntu.ac.ir, granpayeh@kntu.ac.ir (N. Granpayeh).

0030-4018/$ - see front matter © 2013 Elsevier B.V. All rights reserved.
http://dx.doi.org/10.1016/j.optcom.2013.02.037

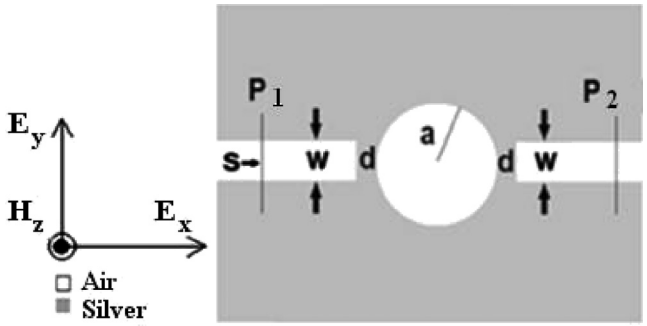

Fig. 1. Schematic view of the basic structure consisted of two separated waveguides with a nanodisk between them. P_1 and P_2 are the input and output powers. a, s, w, and d are the disk radius, source position, waveguide width, and coupling distance, respectively.

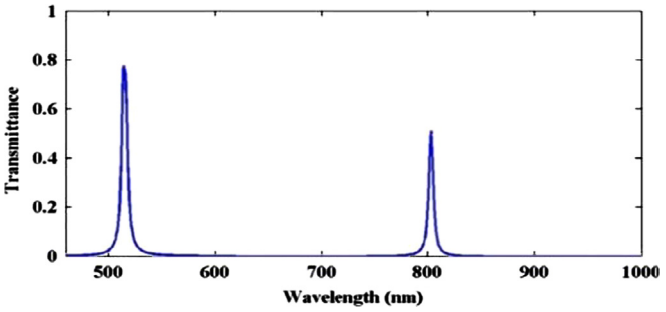

Fig. 2. Spectrum of the transmittance of the structure of Fig. 1 with disk radius of 200 nm and the coupling distance of 30 nm while the width of the waveguides is 50 nm. The wavelengths of the transmission peaks corresponding to the resonance wavelengths of the nanodisk appear at 517.3 nm and 803.4 nm.

fields, by imposing the boundary conditions for tangential magnetic and electric fields at the surrounding surface of the disk, can be expressed as [16]:

$$a_n^i k_d J_n(k_d a) + a_n^s k_d H_n^{(2)}(k_d a) = a_n^t k_m J_n(k_m a) \quad (1)$$

$$\eta_d k_d a_n^i J_n'(k_d a) + \eta_d k_d a_n^s H_n^{(2)\prime}(k_d a) = \eta_m k_m a_n^t J_n'(k_m a) \quad (2)$$

where the subscripts i, s, and t are respectively corresponding to the incident, scattered and transmitted fields. The coefficients a_n^i, a_n^s, and a_n^t are the amplitudes of the incident, scattered and transmitted fields, respectively. η_d and η_m represent the intrinsic impedances of dielectric and metal, respectively. $k_{d,m} = k_0\sqrt{\varepsilon_{d,m}}$ are the wave numbers in the dielectric and metal, k_0 is the free space wave number and ε_d, ε_m, and a are the permittivity of the dielectric, metal, and the radius of the disk, respectively. J_n, $H_n^{(2)}$, J_n', and $H_n^{(2)\prime}$ signify the first kind Bessel function, the second kind Hankel function of the order n and their derivatives, respectively. The metals have been assumed to be silver whose relative permittivity function can be described by Drude model. For the time variation of $e^{j\omega t}$, the model can be expressed as [17]:

$$\varepsilon_m(\omega) = \varepsilon_\infty - \frac{\omega_p^2}{\omega(\omega - j\gamma)} \quad (3)$$

where the material-dependant constants ω_p and γ are the bulk plasma and damping frequencies, respectively, ε_∞ is the dielectric permittivity at the infinite frequency and ω is the angular frequency of the incident lightwave. These parameters for silver are assumed to be $\varepsilon_\infty = 3.7$, $\gamma = 0.018$ eV, and $\omega_p = 9.1$ eV [18].

We can solve Eqs. (1) and (2) for unknown coefficients a_n^t and a_n^s. For a nontrivial solution, the determinant of the matrix of the coefficients must be zero to attain [16]:

$$k_d \frac{H_n^{(2)\prime}(k_m a)}{H_n^{(2)}(k_m a)} = k_m \frac{J_n'(k_d a)}{J_n(k_d a)} \quad (4)$$

The resonance frequencies of a disk with radius a and specified electrical parameters can be obtained from solution of Eq. (4).

3. Simulation results

3.1. General aspects of simulation

In this paper, a two-dimensional FDTD scheme is applied to scrutinize the properties of the structure with the convolutional perfectly matched layers (CPML) absorbing boundary conditions at all boundaries of the simulation domain [18]. The grid sizes in x and y directions are $\Delta x = \Delta y = 5$ nm and the time step, derived by Courant condition is $\Delta t = 0.95/c\sqrt{(\Delta x)^{-2} + (\Delta y)^{-2}}$, where c denotes the speed of light in free space [18]. The incident lightwave for excitation of the SPP mode is a TM_x-polarized plane wave (the magnetic field is parallel to z axis).

3.2. Results and discussions

Fig. 2 shows the transmittance spectrum of the structure. The coupling distance between the waveguides and the nanodisk, the widths of the two waveguides, and the radius of the nanodisk are set to be 20 nm, 30 nm, and 200 nm, respectively. First, the refractive index of the material in the nanodisk, n, is assumed to be 1, which is the refractive index of air. The maximum transmittance occurs at the wavelengths of 803.4 nm and 517.3 nm, corresponding to the first and the second resonance modes of the nanodisk.

Fig. 3 depicts the transmittance spectra of the sensor for different refractive indices of 1 to 1.5 in steps of 0.05. When the refractive index, n, is increased, the resonance wavelengths of the transmitted spectra exhibit red-shift. Fig. 4 displays the linear relationship between the first ($n=1$) and the second ($n=2$) peak wavelengths of the transmittance and the refractive index of the nanodisk material, according to the analytical and simulation results. For example, when the refractive index, n is 1.2, according to Eq. (4) and Fig. 4(a), the resonance wavelength is analytically derived to be 557 nm, which agrees well with the simulated results of 562 nm, shown in Fig. 4(b). With the linear relationship shown in Fig. 4, the refractive index of the material in disk can be obtained from the detected resonance wavelength.

From Fig. 4, it can also be seen that the shift of the second resonance wavelength as a function of the refractive index is equal to 222.2 nm per refractive index unit ($dn/d\lambda = 0.0045\ \text{nm}^{-1}$), whereas the shift of the first resonance wavelength equals 357.1 nm per refractive index unit ($dn/d\lambda = 0.0028\ \text{nm}^{-1}$), which implies that the detection of the shift of the first resonance mode is more suitable for higher resolution sensing. But the power transmission of the first resonance mode is less than that of the second one. Therefore, the designer should consider compromise between the resolution and the level of the detected power.

With the wavelength detection resolution of $\Delta\lambda = 1$ pm, which a high-resolution optical spectrum analyzer can possess it, the sensing resolution of the refractive index sensor, defined as $SR = (dn/d\lambda)\Delta\lambda$, will be 2.8×10^{-6} and 4.5×10^{-6} for the first and the second resonance modes, respectively. So, the sensing resolution will be improved for the first resonance mode. Hence, the SPP refractive-index MIM sensor has high sensitivity, and is appropriate to be used in sensitive biosensor.

Fig. 5 illustrates the resonance wavelengths of the sensor as a function of the nanodisk material refractive index for different radii of the nanodisk of 180, 190, 200, 210, and 220 nm. According to

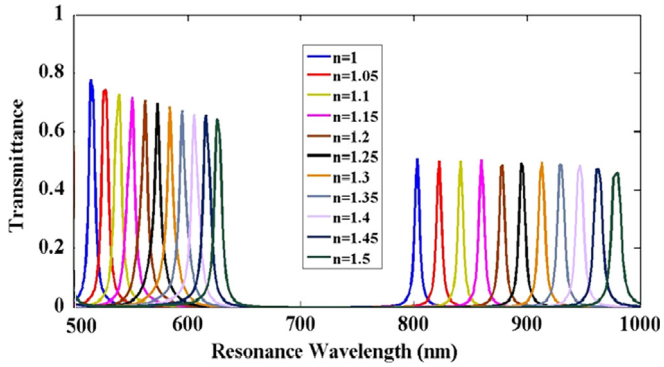

Fig. 3. The transmittance spectra of the structure of Fig. 1 for different refractive indices of 1–1.5.

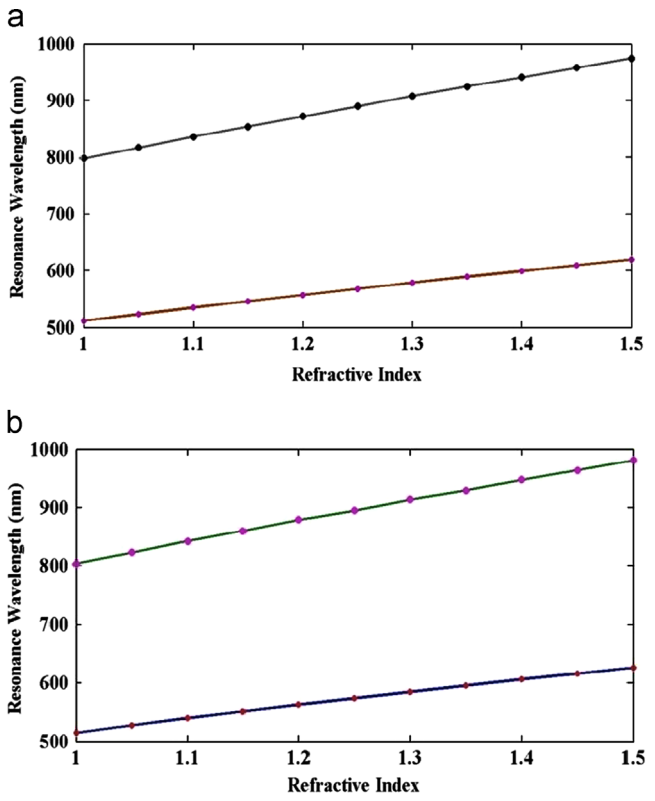

Fig. 4. (a) Theoretical and (b) numerical resonance wavelengths of the structure versus the nanodisk material refractive index for the first and the second resonance modes.

Fig. 5, and by calculating the $dn/d\lambda$, we can plot sensing resolution (SR) versus the disk radius for the first and the second resonance mode (Fig. 6). Fig. 6 depicts that using the first resonance mode, for larger disk, we can reach higher resolution sensor. So, the other compromise can be considered between the size of the disk (structure) and the resolution. As an example, we choose $r=180$ nm, which regarding to Fig. 6, and by detecting the first resonance mode, we can attain a sensor with 3.1×10^{-6} resolution.

Fig. 7 displays the resonance wavelengths of the sensor as a function of the refractive index for different coupling distances. The radius of the disk is set to be 180 nm. The change rate of $dn/d\lambda$ for three different coupling distances of 15, 20 and 25 nm, are approximately 0.0031 nm^{-1} for the first resonance mode. Consequently, the changes in the coupling distances do not affect the resolution of the sensor. However, the higher coupling distances, decrease the power coupling between the nanodisk and the waveguides, and shrink the power transmission.

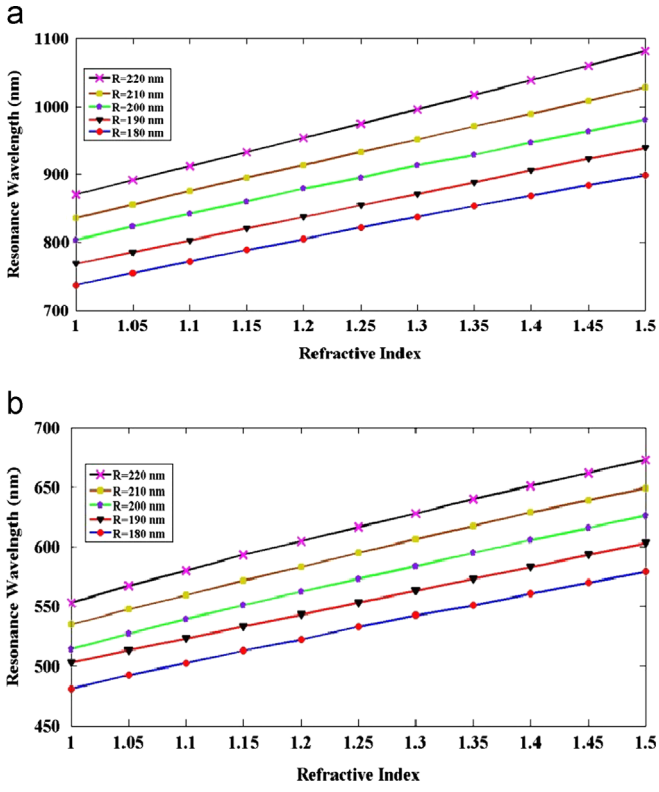

Fig. 5. The resonance wavelengths of the structure versus the nanodisk material refractive index for various disk radii (a) the first and (b) the second resonance mode.

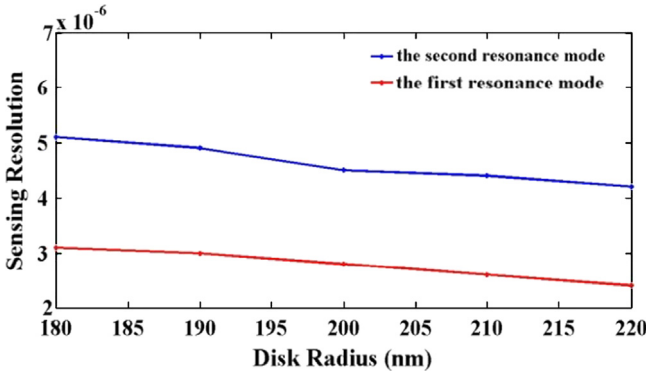

Fig. 6. The sensing resolution versus the disk radius for the first and the second resonance mode.

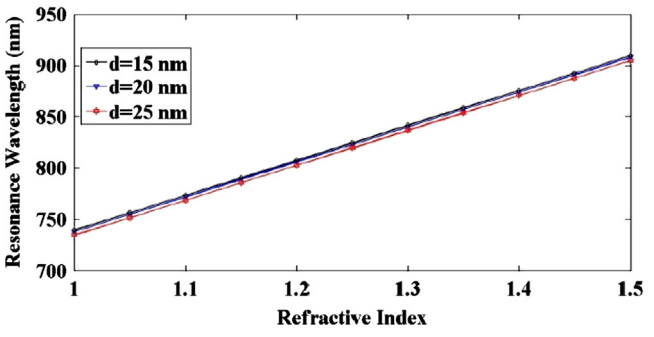

Fig. 7. The resonance wavelength of the first mode versus the refractive index of the nanodisk material for three different coupling distances.

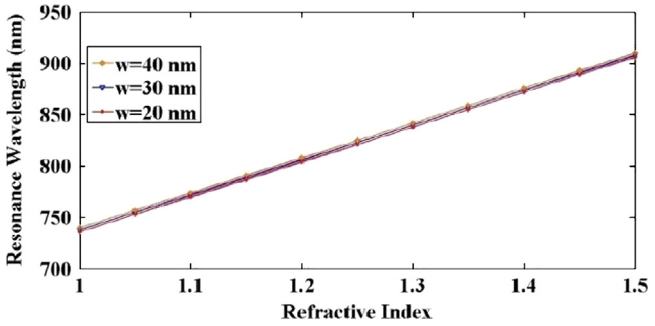

Fig. 8. The resonance wavelength of the first mode versus refractive index of the nanodisk material for three different waveguide widths.

Fig. 8 depicts the first resonance mode wavelengths versus nanodisk material refractive index for three different widths of the waveguide. The variation rate of $dn/d\lambda$ for three different waveguide widths of 20, 30 and 40 nm, are approximately 0.0031 nm^{-1} for the first resonance mode. Again, we can infer that the variations of the widths of the waveguides do not affect the resolution of the sensor. Another compromise can be considered between the lithography techniques for realization of the sensor, and the size of the sensor for using in the photonic integrated circuits (PICs).

For using this sensor, a calibration is required for accurate sensing, before measurement of the refractive index of a material. The calibration could be done in the following steps. First, the sensor is filled up with different materials whose refractive indices are known. Then the first resonance wavelength of the transmittance spectrum is detected. Finally, a calibration curve can be attained from the resonance wavelength versus the refractive indices of different materials. Obviously, the nanodisk should be unpolluted before every measurement. The materials under sensing are supposed not to etch the structure, otherwise it may lead to change of the structural parameters and disturb the calibration.

4. Conclusion

In this paper, a simple plasmonic refractive index sensor is proposed. The resolution can easily be controlled by manipulating the structural parameters. The results were achieved analytically and by the numerical finite difference time domain method. This compact structure has extensive potential in nanoscale industrial sensing, especially as a precise biosensor. It can easily be converted to different useful sensors of temperature, pressure, humidity and concentration of chemicals, based on the refractive index variations by these phenomena through proper designs.

References

[1] W.L. Barnes, A. Darnes, A. Dereux, T.W. Ebbesen, Nature 424 (2003) 824.
[2] Q. Zhang, X.G. Huang, X.S. Lin, J. Tao, X.P. Jin, Optics Express 17 (2009) 7549.
[3] E. Ozbay, Science 311 (2006) 189.
[4] J.J. Mock, D.R. Smith, S. Schultz, Nano Letters 3 (2003) 485.
[5] E.M. Larsson, J. Alegret, M. Kall, D.S. Sutherland, Nano Letters 7 (2007) 1256.
[6] A.G. Brolo, R. Gordon, B. Leathem, K.L. Kavanagh, Langmuir 20 (2004) 4813.
[7] A. Lesuffeur, H. Im, N.C. Lindquist, S.H. Oh, Applied Physics Letters 90 (2007) 243110-1.
[8] J. Ctyrocky, Sensors and Actuators B 54 (1999) 66.
[9] J. Homola, J. Ctyrocky, M. Skalsky, J. Hradilova, P. Kolarova, Sensors and Actuators B 38–39 (1997) 286.
[10] X.P. Jin, X.G. Huang, J. Tao, X.S. Lin, Q. Zhang, A. Novel Nanometric, IEEE Transactions on Nanotechnology 9 (2010) 134.
[11] K. Matsubara, S. Kawata, S. Minami, Applied Optics 27 (1988) 1160.
[12] B. Liedberg, C. Nylander, I. LundstrÖm, Sensors and Actuators B 4 (1991) 299.
[13] A. Schilling, O. Yavaş, J. Bischof, J. Boneborg, P. Leiderer, Applied Physics 69 (1996) 4159.
[14] P. Pfeifer, U. Aldinger, G. Schwotzer, S. Diekman, P. Steinrúcke, Sensors and Actuators B 54 (1999) 166.
[15] J. Homola, S.S. Yee, G. Gauglitz, Sensors and Actuators B 54 (1999) 3.
[16] C.A. Balanis, Advanced Engineering Electromagnetic, Wiley, AZ, USA, 1989.
[17] A. Taflove, S.C. Hagness, Computational Electrodynamics: The Finite-Difference Time-Domain Method, 3rd ed., Artech House, Boston, MA, USA, 2005.
[18] H. Lu, X. Liu, D. Mao, L. Wang, Y. Gong, Optics Express 18 (2010) 17922.